

Structural Characterization of Two New Quaternary Chalcogenides: $\text{CuCo}_2\text{InTe}_4$ and $\text{CuNi}_2\text{InTe}_4$

Gerzon E. Delgado^{a*}, Pedro Grima-Gallardo^b, Luis Nieves^b, Humberto Cabrera^c, Jennifer R. Glenn^d,
Jennifer A. Aitken^d

^a Laboratorio de Cristalografía, Departamento de Química, Facultad de Ciencias, Universidad de Los Andes, Mérida 5101, Mérida, Venezuela

^b Centro de Estudios de Semiconductores, Departamento de Física, Facultad de Ciencias, Universidad de Los Andes, Mérida 5101, Mérida, Venezuela

^c Centro Multidisciplinario de Ciencias, Instituto Venezolano de Investigaciones Científicas – IVIC, Mérida, Mérida, Venezuela

^d Department of Chemistry and Biochemistry, Duquesne University, Pittsburgh, Pennsylvania 15282, United States

Received: February 4, 2016; Revised: August 11, 2016; Accepted: October 2, 2016

The crystal structure of the chalcogenide compounds $\text{CuCo}_2\text{InTe}_4$ and $\text{CuNi}_2\text{InTe}_4$, two new members of the I-II₂-III-VI₄ family, were characterized by Rietveld refinement using X-ray powder diffraction data. Both materials crystallize in the tetragonal space group $I_7 2m$ (No. 121), $Z = 2$, with a stannite-type structure, with the binaries CoTe and NiTe as secondary phases.

Keywords: alloys, semiconductors, chemical synthesis, structural characterization, X-ray powder diffraction

1. Introduction

Diluted magnetic semiconductors (DMS) are of great interest because of their peculiar magnetic and magneto-optical properties arising from the presence of magnetic ions in the lattice¹. The DMS materials more frequently studied are alloys obtained from the tetrahedrally coordinated derivatives of the II-VI semiconductor family². One of these derivative families are the quaternary semiconductors with formula I-II₂-III-VI₄ and I₂-II-IV-VI₄ which belong to the normal compound of fourth derivatives of the II-VI binary semiconductors with three types of cations³, and fulfil the rules of adamantane compound formation^{2,3}. According to these rules, the cation substitution is performed in such a way that an average number of four valence electrons per atomic site and a value eight for the ratio valence electrons to anions is maintained².

Due to the great variety of possible compositions (I= Cu, Ag, II= Zn, Cd, Mn, Fe, III= Al, Ga, In, IV= Si, Ge, Sn, VI= S, Se, Te), these quaternary diamond-like materials can be useful for applications such as tunable semiconductors⁴, photovoltaics⁵, spintronics⁶, non-linear optics⁷ and thermoelectrics⁸. In general, the quaternary compounds I-II₂-III-VI₄ can be formed by the addition of a II-VI binary compound to ternary chalcopyrite structures I-III-VI₂^{9,10}. Structural studies carried out on some members of this family indicate that they crystallize in a sphalerite derivative structure (stannite) with tetragonal space group $I_7 2m$ (No. 121)¹¹, or in a wurtzite derivative structure (wurtzite-

stannite) with orthorhombic space group $Pmn2_1$ (No. 31)¹². This last structure can be considered as a superstructure to wurtzite, where $a \sim 2a_w$, $b \sim \sqrt{3}b_w$, and $c \sim c_w$ ¹².

The quaternaries $\text{CuFe}_2(\text{Al,Ga,In})\text{Se}_4$ ^{13,14}, $\text{CuTa}_2\text{InTe}_4$ ¹⁵, $\text{AgFe}_2\text{GaTe}_4$ ¹⁶ and the stable forms at higher temperatures of $\text{CuZn}_2(\text{Al,Ga,In})\text{S}_4$ ¹⁷, crystallizes in stannite-type structure while $\text{AgCd}_2\text{GaS}_4$ ¹⁸, $\text{AgCd}_2\text{GaSe}_4$ ¹⁹, $\text{Ag}_{1-x}\text{Cu}_x\text{Cd}_2\text{GaS}_4$ ²⁰, $\text{AgCd}_2\text{Ga}_{1-x}\text{In}_x\text{S}_4$ ²¹ and $\text{AgCd}_{2-x}\text{Mn}_x\text{GaS}_4$ ²² have been reported with a wurtz-stannite structure.

In recent years, it has been of interest to carry out a systematic study of the crystal structure of quaternary diamond-like families^{13-16, 23-26}. Hence, in this work we report the X-ray powder diffraction analysis and crystal structure of the quaternary compounds $\text{CuCo}_2\text{InTe}_4$ and $\text{CuNi}_2\text{InTe}_4$, two new members of the I-II₂-III-VI₄ family, which crystallize with a stannite structure.

2. Experimental procedures

2.1. Synthesis

Nominally $\text{CuCo}_2\text{InTe}_4$ and $\text{CuNi}_2\text{InTe}_4$ samples were synthesized using the melt-anneal method. Stoichiometric quantities of Cu, Co, Ni, In, Te elements with purity of at least 99.99% (GoodFellow) were charged in an evacuated synthetic silica glass ampoule, which was previously subjected to pyrolysis in order to avoid reaction of the starting materials with silica glass. Then, the ampoule was sealed under vacuum ($\sim 10^{-4}$ Torr) and the fusion process was carried out inside a furnace (vertical

* e-mail: gerzon@ula.ve

position) heated up to 1500 K at a rate of 20 K/h, with a stop of 48 h at 722.5 K (melting temperature of Te) in order to maximize the formation of binary species at low temperature and minimize the presence of unreacted Te at high temperatures. The ampoule was shaken using a mechanical system during the entire heating process in order to aid the complete mixing of all the elements. The maximum temperature (1500 K) was held for an additional 48 hours with the mechanical shaking system on. Then, the mechanical shaking system was turning off and the temperature was gradually lowered, at the same rate of 20 K/h, until 873 K. The ampoule was held at this temperature for a period of 30 days. Finally, the sample was cooled to room temperature at a rate of 10 K/h. The obtained ingots were bright gray in color and homogeneous to the eye.

2.2. X-ray powder diffraction

X-ray powder diffraction patterns were recorded using a PANalytical X'Pert Pro MPD powder X-ray diffractometer operating in Bragg-Brentano geometry using CuK_α radiation with an average wavelength of 1.5418 Å. A tube power of 45 kV and 40 mA was employed. A nickel filter was used in the diffracted beam optics and the data were collected with the X'Celerator one-dimensional silicon strip detector. A $\frac{1}{4}^\circ$ divergent slit, a $\frac{1}{2}^\circ$ antiscatter slit, and a 0.02 rad soller slit were set at both the incident and diffracted beams. The scan range was from 5 to $145^\circ 2\theta$ with a step size of 0.008° and a scan speed of $0.0106^\circ/\text{s}$.

3. Results and Discussion

Figure 1 and 2 shows the resulting X-ray powder diffractogram for the quaternary compounds $\text{CuCo}_2\text{InTe}_4$ and $\text{CuNi}_2\text{InTe}_4$. An automatic search in the PDF-ICDD database²⁷, using the software available with the diffractometer, indicated that the powder patterns contained important amounts of the binaries CoTe (PDF N° 70-2887) and NiTe (PDF N° 89-2019), respectively.

Bragg positions of the diffraction lines from these binaries are also indicated in Figure 1 and Figure 2. The 20 first peak positions of the main phase, in each case, was indexed using the program Dicvol04²⁸, which gave a unique solution in tetragonal cells with $a = 6.195(2)$ Å, $c = 12.400(4)$ Å for $\text{CuCo}_2\text{InTe}_4$, and $a = 6.160(2)$ Å, $c = 12.365(4)$ Å for $\text{CuCo}_2\text{InTe}_4$.

The systematic absences study ($hkl: h+k+l=2n$) indicated an I-type cell. A revision of the diffraction lines of the main phase taking into account the sample composition, unit cell parameters as well as the body center cell suggested that this material is isostructural with $\text{CuFe}_2\text{InSe}_4$ ¹³ and $\text{AgFe}_2\text{GaTe}_4$ ¹⁶; the firsts of the I-II₂-III-VI₄ family with a stannite structure¹¹, which crystallize in the tetragonal space group I_72m (No. 121). It should be mentioned that Rietveld refinement were performed in the I_7 (No. 82) space group but did not produce a chemically sound structure, ruled out a kesterite structure.

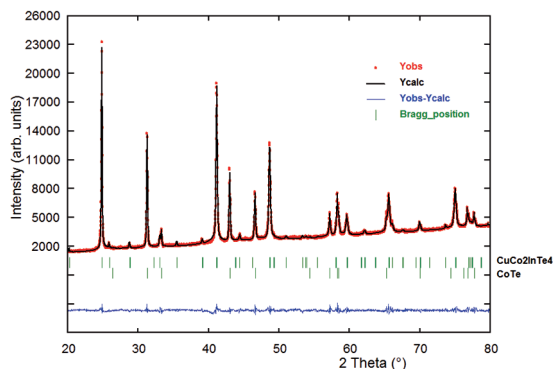


Figure 1: Final Rietveld plot showing the observed, calculated and difference pattern for the $\text{CuCo}_2\text{InTe}_4$ compound. The Bragg reflections for both phases are indicated by vertical bars.

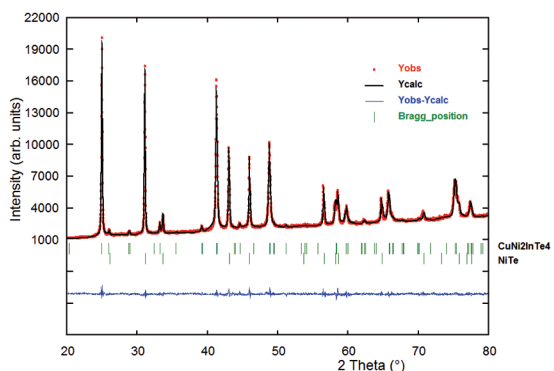


Figure 2: Final Rietveld plot showing the observed, calculated and difference pattern for the $\text{CuNi}_2\text{InTe}_4$ compound. The Bragg reflections for both phases are indicated by vertical bars.

The Rietveld refinement²⁹ of the whole diffraction patterns was carried out using the Fullprof program³⁰, with the unit cell parameters mentioned above. The atomic coordinates of the compound $\text{CuFe}_2\text{InSe}_4$ ¹³ were used as initial model. Atomic positions of the CoTe³¹ and NiTe³² binaries were included as secondary phases in the refinements of $\text{CuCo}_2\text{InTe}_4$ and $\text{CuNi}_2\text{InTe}_4$, respectively.

The angular dependence of the peak full width at half maximum (FWHM) was described by the Caglioti's formula³³. Peak shapes were described by the parameterized Thompson-Cox-Hastings pseudo-Voigt profile function³⁴. The background variation was described by a polynomial with six coefficients. The thermal motion of the atoms was described by one overall isotropic temperature factor. The results of the Rietveld refinement are summarized in Tables 1 and 2. Figures 1 and 2 shows the observed calculated and difference profile for the final cycle of Rietveld refinement in both materials. Atomic coordinates, isotropic temperature factor, bond distances and angles are shown in Tables 3 and 4. The final Rietveld refinement converged to the weight fraction percentages³⁵ shows in Tables 1 and 2. Figure 3 shows the unit cell diagram for the $\text{CuCo}_2\text{InTe}_4$ and $\text{CuNi}_2\text{InTe}_4$ phases.

Table 1: Rietveld refinement results for CuCo₂InTe₄ and CoTe.

Molecular formula	CuCo ₂ InTe ₄	CoTe	
Molecular weight (g/mol)	806.63	186.53	
<i>a</i> (Å)	6.1997(1)	3.8939(1)	
<i>c</i> (Å)	12.380(1)	5.3728(2)	
<i>V</i> (Å ³)	475.84(4)	70.55(1)	
System	tetragonal	hexagonal	
Space group	<i>I</i> -42 <i>m</i> (No. 121)	<i>P</i> 6 ₃ / <i>m</i> <i>m</i> <i>m</i> (No. 194)	
<i>Z</i>	2	2	R _{exp} (%) = 6.7
D _{calc} (g/cm ³)	5.63		R _p (%) = 7.2
Weight fraction (%)	65.2	34.6	R _{wp} (%) = 9.5
R _B (%)	8.5	7.9	S = 1.4
R _{exp} = 100 [(N-P+C) / Σ _w (y _{obs} ²) ^{1/2}]		N-P+C is the number of degrees of freedom	
R _{wp} = 100 [Σ _w y _{obs} - y _{calc} ² / Σ _w y _{obs} ²] ^{1/2}		R _p = 100 Σ y _{obs} - y _{calc} / Σ y _{obs}	
R _B = 100 Σ _k I _k - Ic _k / Σ _k I _k		S = [R _{wp} / R _{exp}]	

Table 2: Rietveld refinement results for CuNi₂InTe₄ and NiTe.

Molecular formula	CuNi ₂ InTe ₄	NiTe	
Molecular weight (g/mol)	806.15	186.29	
<i>a</i> (Å)	6.1669(1)	3.9411(2)	
<i>c</i> (Å)	12.370(1)	5.3177(3)	
<i>V</i> (Å ³)	470.44(4)	71.53(1)	
System	tetragonal	hexagonal	
Space group	<i>I</i> -42 <i>m</i> (No. 121)	<i>P</i> 6 ₃ / <i>m</i> <i>m</i> <i>m</i> (No. 194)	
<i>Z</i>	2	2	R _{exp} (%) = 6.5
D _{calc} (g/cm ³)	5.69		R _p (%) = 7.2
Weight fraction (%)	58.3	41.7	R _{wp} (%) = 9.6
R _B (%)	8.7	8.0	S = 1.5
R _{exp} = 100 [(N-P+C) / Σ _w (y _{obs} ²) ^{1/2}]		N-P+C is the number of degrees of freedom	
R _{wp} = 100 [Σ _w y _{obs} - y _{calc} ² / Σ _w y _{obs} ²] ^{1/2}		R _p = 100 Σ y _{obs} - y _{calc} / Σ y _{obs}	
R _B = 100 Σ _k I _k - Ic _k / Σ _k I _k		S = [R _{wp} / R _{exp}]	

Table 3: Atomic coordinates, isotropic temperature factor, bond distances (Å) and angles (°) for CuCo₂InTe₄.

Atom	Ox.	Wyck.	<i>x</i>	<i>y</i>	<i>z</i>	Foc	B (Å ²)
Cu	+1	2 <i>a</i>	0	0	0	1	0.31(5)
Co	+2	4 <i>d</i>	0	½	¼	1	0.31(5)
In	+3	2 <i>b</i>	0	0	½	1	0.31(5)
Te	-2	8 <i>i</i>	0.264(1)	0.264(1)	0.124(1)	1	0.31(5)
Cu - Te ⁱ	2.576(9)		Co - Te	2.693(9)		In - Te	2.777(9)
Te - Cu - Te ⁱⁱ	106.9(2)	x4	Te - Co - Te ^{iv}	109.6(2)	x4	Te ⁱ - In - Te ^{iv}	107.8(2) x4
Te - Cu - Te ⁱⁱⁱ	110.6(2)	x2	Te - Co - Te ^v	109.2(2)	x2	Te ^{iv} - In - Te ^{vi}	112.7(2) x2

Symmetry codes: (i) -0.5+x, -0.5+y, 0.5+z; (ii) -y, x, -z; (iii) -x, -y, z; (iv) -0.5+y, 0.5-x, 0.5-z; (v) -x, 1-y, z; (vi) 0.5-y, -0.5+x, 0.5-z.

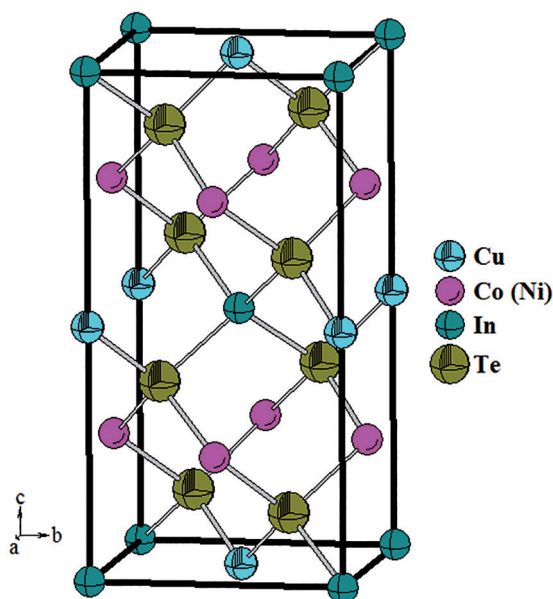
Quaternary CuCo₂InTe₄ and CuNi₂InTe₄ are normal adamantane-structure compound and can be described as derivative of the sphalerite with a stannite-type structure². As expected for adamantane structure compounds, each anion is coordinated by four cations (two Co or Ni, one Cu and one In) located at the corners of a slightly distorted tetrahedron. Cu, Co (Ni) and In cations are similarly

coordinated by four anions. The interatomic distances are shorter than the sum of the respective ionic radii for structures tetrahedrally bonded³⁶. The Cu-Te, Co-Te, Ni-Te and In-Te bond distances are in good agreement with those observed in other adamantane structure compounds found in the ICSD database³⁷; such as CuTa₂InTe₄¹⁵, CuInTe₂³⁸, AgIn₅Te₈³⁹, Cu₃NbTe₄⁴⁰ and AgInTe₂⁴¹.

Table 4: Atomic coordinates, isotropic temperature factor, bond distances (Å) and angles (°) for $\text{CuNi}_2\text{InTe}_4$.

Atom	Ox.	Wyck.	x	Y	z	Foc	B (Å ²)
Cu	+1	2a	0	0	0	1	0.23(5)
Ni	+2	4d	0	½	¼	1	0.23(5)
In	+3	2b	0	0	½	1	0.23(5)
Te	-2	8i	0.264(1)	0.264(1)	0.125(1)	1	0.23(5)
Cu - Te ⁱ	2.574(9)	Ni - Te	2.676(9)	In - Te	2.773(9)		
Te - Cu - Te ⁱⁱ	106.2(2) x4	Te - Ni - Te ^{iv}	109.5(2) x4	Te ⁱ - In - Te ^{iv}	108.1(2) x4		
Te - Cu - Te ⁱⁱⁱ	111.2(2) x2	Te - Ni - Te ^v	109.4(2) x2	Te ^{iv} - In - Te ^{vi}	112.2(2) x2		

Symmetry codes: (i) $-0.5+x, -0.5+y, 0.5+z$; (ii) $-y, x, -z$; (iii) $-x, -y, z$; (iv) $-0.5+y, 0.5-x, 0.5-z$; (v) $-x, 1-y, z$; (vi) $0.5-y, -0.5+x, 0.5-z$.

**Figure 3:** Unit cell diagram for the $\text{CuCo}_2\text{InTe}_4$ and $\text{CuNi}_2\text{InTe}_4$ phases.

4. Conclusions

The crystal structure of the quaternary compounds $\text{CuCo}_2\text{InTe}_4$ and $\text{CuNi}_2\text{InTe}_4$ was determined using X-ray powder diffraction. $\text{CuCo}_2\text{InTe}_4$ and $\text{CuNi}_2\text{InTe}_4$ crystallize in the tetragonal space group $I7_2m$ with a stannite-type structure.

5. Acknowledgments

Authors want to thank to CDCHTA-ULA (grant C-1885-14-05-B) and FONACIT (grants 2011001341 and LAB-97000821).

6. References

- Nikiforov KG. Magnetically ordered multinary semiconductors. *Progress in Crystal Growth and Characterization of Materials*. 1999;39(1-4):1-104. [http://dx.doi.org/10.1016/S0960-8974\(99\)00016-9](http://dx.doi.org/10.1016/S0960-8974(99)00016-9)
- Parthé E. Wurtzite and Zinc-Blend Structures. In: Westbrook JH, Fleischer RL, Eds. *Intermetallic compounds, principles and applications*. Vol 1, Chap. 14. Hoboken: John Wiley & Sons; 1995.
- Delgado JM. Crystal chemistry of diamond-like and other derivative semiconducting compounds. *Journal of Physics: Conference Series*. 1998;152:45-50.
- Ford GM, Guo Q, Agrawal R, Hillhouse HW, Hugh W. Earth abundant element $\text{Cu}_2\text{Zn}(\text{Sn}_{1-x}\text{Ge}_x)_4\text{S}_4$ nanocrystals for tunable band gap solar cells: 6.8% efficient device fabrication. *Chemistry of Materials*. 2011;23(10):2626-2629. <http://dx.doi.org/10.1021/cm2002836>
- Guo Q, Ford GM, Yang WC, Walker BC, Stach EA, Hillhouse HW, et al. Fabrication of 7.2% efficient CZTSSe solar cells using CZTS nanocrystals. *Journal of American Chemical Society*. 2010;132(49):17384-17386. <http://dx.doi.org/10.1021/ja108427b>
- Chambers SA, Yoo YK. New materials for spintronics. *MRS Bulletin*. 2003;28:706-710. <http://dx.doi.org/10.1557/mrs2003.210>
- Li Y, Fan W, Sun H, Cheng X, Li P, Zhao X. Electronic, optical and lattice dynamic properties of the novel diamond-like semiconductors $\text{Li}_2\text{CdGeS}_4$ and $\text{Li}_2\text{CdSnS}_4$. *Journal of Physics: Condensed Matter*. 2011;23(22):225401. <http://dx.doi.org/10.1088/0953-8984/23/22/225401>
- Sevik C, Çağın T. *Ab initio* study of thermoelectric transport properties of pure and doped quaternary compounds. *Physical Review B*. 2010;82(4):045202. <http://dx.doi.org/10.1103/PhysRevB.82.045202>
- Grima-Gallardo P, Cárdenas K, Molina L, Quintero M, Ruiz J, Delgado GE, et al. A comparative study of $(\text{Cu-III-Te}_2)_x(\text{FeSe})_{1-x}$ alloys (III : Al, Ga, In) ($0 \leq x \leq 1$) by X-ray diffraction (XRD), differential thermal analysis (DTA) and scanning electron microscopy (SEM). *Physica Status Solidi (a)*. 2001;187(2):395-406. [http://dx.doi.org/10.1002/1521-396X\(200110\)187:2<395::AID-PSSA395>3.0.CO;2-2](http://dx.doi.org/10.1002/1521-396X(200110)187:2<395::AID-PSSA395>3.0.CO;2-2)
- Grima-Gallardo P, Cárdenas K, Quintero M, Ruiz J, Delgado G. X-ray diffraction (XRD) studies on $(\text{CuAlSe}_2)_x(\text{FeSe})_{1-x}$ alloys. *Materials Research Bulletin*. 2001;36(5-6):861-866. [http://dx.doi.org/10.1016/S0025-5408\(01\)00546-3](http://dx.doi.org/10.1016/S0025-5408(01)00546-3)
- Hall SR, Szymanski JT, Stewart JM. Kesterite, $\text{Cu}_2(\text{Zn,Fe})\text{SnS}_4$, and stannite, $\text{Cu}_2(\text{Fe,Zn})\text{SnS}_4$, structurally similar but distinct minerals. *Canadian Mineralogist*. 1978;16:131-137. <http://canmin.geoscienceworld.org/content/16/2/131.extract>
- Parthé E, Yvon K, Deitch RH. The crystal structure of $\text{Cu}_2\text{CdGeS}_4$ and other quaternary normal tetrahedral structure compounds. *Acta Crystallographica B*. 1969;25:1164-1174. <http://dx.doi.org/10.1107/S0567740869003670>

13. Delgado GE, Mora AJ, Grima-Gallardo P, Quintero M. Crystal structure of $\text{CuFe}_2\text{InSe}_4$ from X-ray powder diffraction. *Journal of Alloys and Compounds*. 2008;454(1-2):306-309. <http://dx.doi.org/10.1016/j.jallcom.2006.12.057>
14. Delgado GE, Mora AJ, Grima-Gallardo P, Muñoz M, Durán S, Quintero M, et al. Crystal structure of the quaternary compounds $\text{CuFe}_2\text{AlSe}_4$ and $\text{CuFe}_2\text{GaSe}_4$ from X-ray powder diffraction. *Bulletin of Materials Science*. 2015;38(4):1061-1064. <http://dx.doi.org/10.1007/s12034-015-0933-9>
15. Delgado GE, Mora AJ, Grima-Gallardo P, Muñoz M, Durán S, Quintero M. Crystal structure of the quaternary compound $\text{CuTa}_2\text{InTe}_4$ from X-ray powder diffraction. *Physica B: Condensed Matter*. 2008;403(18):3228-3230. <http://dx.doi.org/10.1016/j.physb.2008.04.022>
16. Delgado GE, Quintero E, Tovar R, Grima-Gallardo P, Quintero M. Synthesis and crystal structure of the quaternary compound $\text{AgFe}_2\text{GaTe}_4$. *Journal of Alloys and Compounds*. 2014;613:143-145. <http://dx.doi.org/10.1016/j.jallcom.2014.06.004>
17. Ghosh A, Palchoudhury S, Thangavel R, Zhou Z, Naghibolashrafi N, Ramasamy K, et al. A new family of wurtzite-phase $\text{Cu}_2\text{ZnAS}_{4-x}$ and CuZn_2AS_4 (A= Al, Ga, In) nanocrystals for solar energy conversion applications. *Chemical Communications*. 2016;52:264-267. <http://dx.doi.org/10.1039/C5CC07743E>
18. Chykhrij SI, Parasyuk OV, Halka OV. Crystal structure of the new quaternary phase $\text{AgCd}_2\text{GaS}_4$ and phase diagram of the quasi-binary system AgGaS_2 - CdS . *Journal of Alloys and Compounds*. 2000;312(1-2):189-195. [http://dx.doi.org/10.1016/S0925-8388\(00\)01145-2](http://dx.doi.org/10.1016/S0925-8388(00)01145-2)
19. Olekseyuk ID, Gulay LD, Parasyuk OV, Husak OA, Kadykalo EM. Phase diagram of the AgGaSe_2 - CdSe system and crystal structure of the $\text{AgCd}_2\text{GaSe}_4$ compound. *Journal of Alloys and Compounds*. 2002;343(1-2):125-131. [http://dx.doi.org/10.1016/S0925-8388\(02\)00143-3](http://dx.doi.org/10.1016/S0925-8388(02)00143-3)
20. Zmiy OF, Mishchenko IA, Olekseyuk ID. Phase equilibria in the quasi-ternary system Cu_2Se - CdSe - In_2Se_3 . *Journal of Alloys and Compounds*. 2004;367(1-2):49-57. <http://dx.doi.org/10.1016/j.jallcom.2003.08.011>
21. Olekseyuk ID, Parasyuk OV, Husak OA, Piskach LV, Volkov SV, Pekhnyo VI. X-ray powder diffraction study of semiconducting alloys $\text{Ag}_{1-x}\text{Cu}_x\text{Cd}_2\text{GaS}_4$ and $\text{AgCd}_2\text{Ga}_{1-x}\text{In}_x\text{S}_4$. *Journal of Alloys and Compounds*. 2005;402(1-2):186-193. <http://dx.doi.org/10.1016/j.jallcom.2005.04.147>
22. Davydyuk GY, Sachanyuk VP, Voronyuk SV, Olekseyuk ID, Romanyuk YE, Parasyuk OV. X-ray diffraction study of the $\text{AgCd}_{2-x}\text{Mn}_x\text{GaS}_4$ semiconductor alloys and their electrical, optical, and photoelectrical properties. *Physica B: Condensed Matter*. 2006;373(2):355-359. <http://dx.doi.org/10.1016/j.physb.2005.12.249>
23. Mora AJ, Delgado GE, Grima-Gallardo P. Crystal structure of CuFeInSe_4 from X-ray powder diffraction data. *Physica Status Solidi (a)*. 2007;204(2):547-554. <http://dx.doi.org/10.1002/pssa.200622395>
24. Delgado GE, Mora AJ, Grima-Gallardo P, Durán S, Muñoz M, Quintero M. Crystal structure of the quaternary alloy CuTaInSe_4 . *Crystal Research & Technology*. 2008;43(7):783-785. <http://dx.doi.org/10.1002/crat.200711154>
25. Delgado GE, Mora AJ, Contreras JE, Grima-Gallardo P, Durán S, Muñoz M, et al. Crystal structure characterization of the quaternary compounds CuFeAlSe_3 and CuFeGaSe_3 . *Crystal Research and Technology*. 2009;44(5):548-552. <http://dx.doi.org/10.1002/crat.200800596>
26. Delgado GE, Mora AJ, Grima-Gallardo P, Durán S, Muñoz M, Quintero M. Preparation and crystal structure characterization of CuNiGaSe_3 and CuNiInSe_3 quaternary compounds. *Bulletin of Materials Science*. 2010;33(5):637-640. <http://dx.doi.org/10.1007/s12034-010-0097-6>
27. International Centre for Diffraction Data. *PDF-ICDD-Powder Diffraction File (Set 1-65)*. Newtown Square: International Centre for Diffraction Data; 2013.
28. Boultif A, Löuer D. Powder pattern indexing with the dichotomy method. *Journal of Applied Crystallography*. 2004;37:724-731. <http://dx.doi.org/10.1107/S0021889804014876>
29. Rietveld HM. A profile refinement method for nuclear and magnetic structures. *Journal of Applied Crystallography*. 1969;2:65-71. <http://dx.doi.org/10.1107/S0021889869006558>
30. Rodríguez-Carvajal J. Recent advances in magnetic structure determination by neutron powder diffraction. *Physica B: Condensed Matter*. 1993;192(1-2):55-69. [http://dx.doi.org/10.1016/0921-4526\(93\)90108-I](http://dx.doi.org/10.1016/0921-4526(93)90108-I)
31. de Meester de Betzembroeck P, Naud J. Étude par diffraction-X de quelques composés du système Ni-Co-Te obtenus par synthèse thermique. *Bulletin des Sociétés Chimiques Belges*. 1971;80(1-2):107-116. <http://dx.doi.org/10.1002/bscb.19710800112>
32. Røst E, Vestersjø E. On the system Ni-Se-Te. *Acta Chemica Scandinavica*. 1968;22:2118-2134.
33. Cagliotti G, Paoletti A, Ricci FP. Choice of collimators for a crystal spectrometer for neutron diffraction. *Nuclear Instruments*. 1958;3(4):223-228. [http://dx.doi.org/10.1016/0369-643X\(58\)90029-X](http://dx.doi.org/10.1016/0369-643X(58)90029-X)
34. Thompson P, Cox DE, Hastings JB. Rietveld refinement of Debye-Scherrer synchrotron X-ray data from Al_2O_3 . *Journal of Applied Crystallography*. 1987;20:79-83. <http://dx.doi.org/10.1107/S0021889887087090>
35. Hill RJ, Howard CJ. Quantitative phase analysis from neutron powder diffraction data using the Rietveld method. *Journal of Applied Crystallography*. 1987;20:467-474. <http://dx.doi.org/10.1107/S0021889887086199>
36. Shannon RD. Revised effective ionic radii and systematic studies of interatomic distances in halides and chalcogenides. *Acta Crystallographica A*. 1976;32:751-767. <http://dx.doi.org/10.1107/S0567739476001551>
37. Gemlin Institute. ICSD - Inorganic Crystal Structure Database. Scientific Manual. Karlsruhe: Gemlin Institute; 2008. Available from: <https://www.nist.gov/sites/default/files/documents/srd/09-0303-sci_man_ICSD_v1.pdf>. Access in: 10/10/2016.
38. Knight KS. The crystal structures of CuInSe_2 and CuInTe_2 . *Materials Research Bulletin*. 1992;27(2):161-167. [http://dx.doi.org/10.1016/0025-5408\(92\)90209-I](http://dx.doi.org/10.1016/0025-5408(92)90209-I)
39. Mora AJ, Delgado GE, Pineda C, Tinoco T. Synthesis and structural study of the AgIn_3Te_8 compound by X-ray powder diffraction. *Physica Status Solidi (a)*. 2004;201(7):1477-1483. <http://dx.doi.org/10.1002/pssa.200406805>

40. Delgado GE, Mora AJ, Grima-Gallardo P, Durán S, Muñoz M, Quintero M. Synthesis and characterization of the ternary chalcogenide compound Cu_3NbTe_4 . *Chalcogenide Letters*. 2009;6(8):335-338. http://www.chalcogen.ro/335_Delgado.pdf
41. Delgado GE, Mora AJ, Pineda, Ávila-Godoy R, Paredes-Dugarte S. X-ray powder diffraction data and rietveld refinement of the ternary semiconductor chalcogenides AgInSe_2 and AgInTe_2 . *Revista Latinoamericana de Metalurgia y Materiales*. 2015;35(1):110-117. <http://www.rlmm.org/ojs/index.php/rlmm/article/view/546>